Click Here for Full Article

Fractional advection-dispersion equations for modeling transport at the Earth surface

Rina Schumer,[1] Mark M. Meerschaert,[2] and Boris Baeumer[3]

[1] Characterizing the collective behavior of particle transport on the Earth surface is a key ingredient in describing landscape evolution. We seek equations that capture essential features of transport of an ensemble of particles on hillslopes, valleys, river channels, or river networks, such as mass conservation, superdiffusive spreading in flow fields with large velocity variation, or retardation due to particle trapping. Development of stochastic partial differential equations such as the advection-dispersion equation (ADE) begins with assumptions about the random behavior of a single particle: possible velocities it may experience in a flow field and the length of time it may be immobilized. When assumptions underlying the ADE are relaxed, a fractional ADE (fADE) can arise, with a non-integer-order derivative on time or space terms. Fractional ADEs are nonlocal; they describe transport affected by hydraulic conditions at a distance. Space fractional ADEs arise when velocity variations are heavy tailed and describe particle motion that accounts for variation in the flow field over the entire system. Time fractional ADEs arise as a result of power law particle residence time distributions and describe particle motion with memory in time. Here we present a phenomenological discussion of how particle transport behavior may be parsimoniously described by a fADE, consistent with evidence of superdiffusive and subdiffusive behavior in natural and experimental systems.

Citation: Schumer, R., M. M. Meerschaert, and B. Baeumer (2009), Fractional advection-dispersion equations for modeling transport at the Earth surface, *J. Geophys. Res.*, *114*, F00A07, doi:10.1029/2008JF001246.

1. Introduction

[2] An important class of problems in the Earth surface sciences involves describing the collective behavior of particles in transport. Familiar examples include transport of solute and contaminant particles in surface and subsurface water flows, the behavior of soil particles and associated soil constituents undergoing biomechanical transport and mixing by bioturbation, and the transport of sediment particles and sediment-borne substances in turbulent shear flows, whether involving shallow flows over soils, deeper river flows, or ocean currents. These and many other examples share three essential features. First, is the behavior of a well defined ensemble of particles. These particles may be considered "tracers" whose total mass is conserved or otherwise accounted for if radioactive decay, physical transformations or chemical reactions are involved. Second, these tracers typically alternate between states of motion and rest over many time scales, and indeed, most tracers of interest in Earth surface systems are at rest much of the time. Third, when in transport, some tracers move faster, and some move slower,

than the average motion due to spatiotemporal variations in the mechanisms inducing their motion. Tracer motions thus may be considered as consisting of quasi-random walks with rest periods.

[3] During motion, tracers may experience characteristically different "hop" or "jump" behaviors. Consider releasing at some instant an ensemble of tracers within a system, say, marked particles within a river. Assuming all tracers undergo and remain in motion, then due to turbulence fluctuations in the case of suspended particles, or to effects of near-bed turbulence excursions together with tracer-bed interactions in the case of bed load particles, during a small interval of time Δt, most of the tracers move short distances downstream whereas a few move longer distances. The displacement (or hop) distance Δx generally may be considered a random variable. If the probability density function (pdf) describing hop length has a form that declines at least as fast as an exponential distribution, then it possesses finite mean and variance. Moreover, after finite time t, the center of mass of the tracers is centered at the position $x = x_0 + vt$, where x_0 is the starting position and v is the mean tracer speed. The spread or "dispersion" around average tracer position, described by standard deviation, grows at a constant rate with time $\sigma = (Dt)^{1/2}$ where D is the dispersion coefficient. As described below, this behavior, know as Fickian or Boltzmann scaling, may be characterized as being "local," in that during a small interval, tracers in motion mostly move from location x to nearby positions. Conversely, during the same interval, tracers arriving at position x mostly originate

[1]Division of Hydrologic Sciences, Desert Research Institute, Reno, Nevada, USA.
[2]Department of Statistics and Probability, Michigan State University, East Lansing, Michigan, USA.
[3]Department of Mathematics and Statistics, University of Otago, Dunedin, New Zealand.

from nearby positions. Letting $C(x, t)$ denote the local tracer concentration, then in this local case the behavior of C may be adequately described by the classic advection-dispersion equation (ADE).

[4] Consider, in contrast, the possibility that the hop length pdf declines with distance in such a way that the variance is undefined, for example, a power law distribution. In this case, long displacement distances, albeit relatively rare, are nonetheless more numerous than with, say, an exponential distribution, so that hop length density possesses a so-called "heavy tail." For example, during downstream transport, sediment tracers dispersed by turbulent eddies and by momentary excursions into parts of the mean flow that are either faster or slower than the average may occasionally experience "superdispersive" events during excursions into sites with unusually high flow velocities [*Bradley et al.*, 2009]. In these situations where the hop length density is heavy tailed, the scaling of dispersion is non-Fickian, that is, $\sigma = (Dt)^{1/\alpha}$, where $1 < \alpha < 2$. Because σ therefore grows at a rate faster than "normal" Fickian dispersion, this behavior is referred to as superdiffusive. Moreover, this behavior may be characterized as being "nonlocal" in that during a small interval, tracers released from position x mostly move to nearby positions, but also involve an "unusually large" number of motions to positions far from x. Conversely, during the same interval, tracers arriving at position x mostly originate from nearby positions, but also involve a significant number or motions originating far from x. This means that the behavior at a particular position does not necessarily depend only on local (nearby) conditions, but rather may also depend on conditions upstream or downstream. For example, because the local rate of change in tracer concentration consists of the divergence of the flux of tracers, then if the flux is related to the bed stress, say, in the case of sediment transport, the possibility exists that changes in the local concentration depend on stress conditions, and therefore on system configuration, "far" upstream. As described below, the behavior of the tracer concentration $C(x, t)$ in this nonlocal case may be described by a fractional derivative version of the advection-dispersion equation.

[5] Consider now an ensemble of tracers whose motions, after release, involve states of motion and rest. In the case of tracer particles moving as bed load, rest states might involve momentary disentrainment on the bed surface associated with turbulence fluctuations, or burial beneath the surface for longer periods followed by reentrainment with scour [*Nikora et al.*, 2002; *Parker et al.*, 2000]. Even longer rest periods might consist of storage of tracers within the bars and floodplain of a river [*Malmon et al.*, 2002, 2003]. Similarly, rest times of nutrients in open-channel flow might consist of temporary excursions into so-called dead zones, or into hyporheic zone storage, with eventual release back into the main fluid column [*Haggerty et al.*, 2002; *Gooseff et al.*, 2003]. With bioturbation of soil particles, rest times consist of the intervals between displacement by biotic activity. The rest time (or waiting time, or residence time) may be considered a random variable. If random waiting times are, in general, small, then the speed V may be considered an average "virtual speed" that includes periods of motion and rest, and the local rate of change in tracer concentration, $\frac{\partial C}{\partial t}$, in the ADE accommodates this. If, in contrast the waiting time density is a heavy-tailed distribu-

tion that reflects the presence of unusually "long" rest periods for tracers in storage, then as described below a suitable phenomenological description of the behavior of the tracer concentration $C(x, t)$ may be obtained from a fractional ADE (fADE) with a fractional time term $\frac{\partial^{\gamma} C}{\partial t^{\gamma}}$, where $0 < \gamma < 1$. Dispersion now scales at a rate proportional to $t^{\gamma/2}$. Because σ grows at a rate slower than normal Fickian dispersion, this behavior is referred to as "subdiffusion." This characterizes a "long memory" effect, analogous to an influence from far upstream as described above with reference to the fractional space derivative; the fractional time derivative characterizes an influence from far back in time. Like variations in tracer speed, rest times contribute to dispersion. As such, these effects may not be separable without ancillary information.

[6] As elaborated below, if both the hop length density and the waiting time density are heavy tailed, then the fADE can include both a time and a space fractional derivative. Dispersion now scales at a rate proportional to $t^{\gamma/\alpha}$. Note that a particular value of the ratio $\frac{\gamma}{\alpha}$ is a nonunique combination of values of α and γ. This means that if the ratio is obtained empirically from measurements of tracer dispersion, say, in a flume or river, additional information, empirical and/or theoretical, is needed to distinguish whether the source of the anomalous dispersion resides with the hop lengths, waiting times, or both. On this note we point out that the development below provides a mostly phenomenological viewpoint of how tracer behavior may be parsimoniously described by a fADE, consistent with evidence of superdiffusive and subdiffusive behavior in natural and experimental systems [e.g., *Benson et al.*, 2001, 2000a, 2000b; *Haggerty et al.*, 2002; *Schumer et al.*, 2003]. A particularly exciting opportunity resides in clarifying the underlying physics that lead to these behaviors, including the mechanisms that give rise to heavy tail distributions of hop distances and waiting times, perhaps building on recent insights from the hydrologic literature. In section 3, we look at details underlying the application of fractional advection-dispersion equations for describing collective behavior of particle transport at the Earth surface. Much of this manuscript is a review of basic information about fADE for nonspecialists that is not available in a single reference. New material fills in theoretical gaps, compares solution characteristics and application of various fADEs, and links landscape evolution processes to the conceptual models underlying fADEs.

2. Fractional Derivatives

[7] Before presenting fractional ADEs, we provide some useful introductory material about fractional derivatives. Three characteristics of fractional derivatives will be used to interpret and solve fractional ADEs: (1) the Grunwald fractional difference quotient that approximates a fractional derivative; (2) the fractional derivative as the convolution of an integer-order derivative with a memory function; and (3) the Fourier and Laplace transforms of fractional derivatives.

2.1. Grunwald Finite Difference

[8] How can we generalize our understanding of derivatives to include non-integer-order cases? The first derivative of a function $y = f(x)$ is approximated by the difference quotient
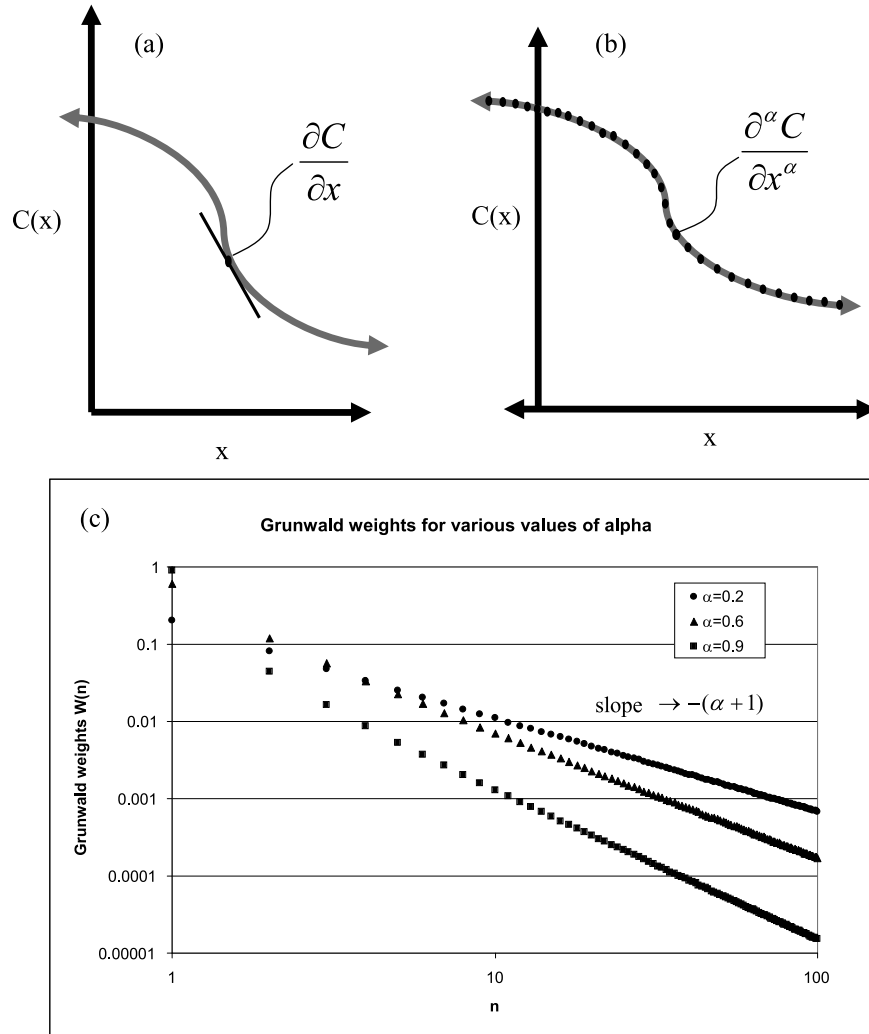
Figure 1. (a) The usual derivative is local, but (b) the fractional derivative is nonlocal. (c) The log-log plot demonstrates the power law decay in Grunwald weights.

$\Delta y/\Delta x$ where $\Delta x = h$ and $\Delta y = f(x) - f(x - h)$ (Figure 1a). The second derivative $f''(x)$ is approximated by $\Delta^2 y/\Delta x^2$ where

$$
\begin{aligned}
\Delta^2 y &= \Delta[f(x) - f(x - h)] \\
&= [f(x) - f(x - h)] - [f(x - h) - f(x - 2h)] \\
&= f(x) - 2f(x - h) + f(x - 2h)
\end{aligned} \tag{1}
$$

the second difference. Continuing in this manner shows that the nth-order derivative is approximated by the nth finite difference quotient

$$
\frac{d^n}{dx^n} f(x) \approx \frac{1}{h^n} \sum_{j=0}^{n} \binom{n}{j}(-1)^j f(x - jh), \tag{2}
$$

where the binomial coefficients (from Pascal's triangle)

$$
\binom{n}{j} \frac{n!}{j!(n-j)!} = \frac{\Gamma(n+1)}{\Gamma(j+1)\Gamma(n-j)}.
$$

The Grunwald definition of the fractional derivative is the noninteger variant of (2)

$$
\frac{d^\alpha}{dx^\alpha} f(x) \approx \frac{1}{h^\alpha} \sum_{j=0}^{\infty} \binom{\alpha}{j}(-1)^j f(x - jh), \tag{3}
$$

where the fractional binomial coefficients are

$$
\binom{\alpha}{j} = \frac{\Gamma(\alpha+1)}{\Gamma(j+1)\Gamma(\alpha-j)}
$$

and the approximation becomes exact as $h = \Delta x \to 0$. To see that the integer-order formula (2) is really a special case of the fractional formula (3), note that the binomial coefficients are $0 = 1/\infty$ for $j > n$, so that we could have written the sum in (2) with the upper limit of infinity.

[9] Several interesting properties of the fractional derivative follow from the Grunwald definition (3). Most important is that a fractional derivative is a nonlocal operator that

depends on function values far away from x (Figure 1b). The importance given to a far away point $x - jh$ is measured by the Grunwald weight $w_j = (-1)^j \Gamma(\alpha + 1)/(\Gamma(j + 1) \cdot \Gamma(\alpha - j))$ so that $w_0 = 1$, $w_1 = -\alpha$, $w_2 = \alpha(\alpha - 1)/2$ and $w_{j+1} = w_j \cdot (j - \alpha)/(j + 1)$. An appeal to Stirling's approximation [*Meerschaert and Scheffler*, 2002] shows that $w_j \approx j^{-(1+\alpha)}/\Gamma(-\alpha)$ (Figure 1). Hence the Grunwald definition is essentially a discrete convolution with a power law. The finite difference formula (3) is also the basis for numerical codes to solve the fractional ADE [*Tadjeran et al.*, 2006].

2.2. Convolution of the Derivative With a Power Law Memory Function

[10]　The continuum limit of the Grunwald finite difference formula is a convolution integral [see, e.g., *Meerschaert and Tadjeran*, 2004]. Writing (3) in terms of the Grunwald weights and using $w_j \approx j^{-(1+\alpha)}/\Gamma(-\alpha)$ suggests

$$\frac{d^\alpha}{dx^\alpha} f(x) \approx \frac{1}{\Gamma(-\alpha)} \sum_{j=0}^{\infty} f(x - jh)(jh)^{-\alpha-1} h$$

$$\approx \frac{1}{\Gamma(-\alpha)} \int_0^\infty f(x - y) y^{-\alpha-1} \, dy \qquad (4)$$

which can be written in various equivalent forms [*Samko et al.*, 1993; *Mainardi*, 1997]. If $f(t)$ is defined on $t \geq 0$ then integration by parts yields the Caputo form

$$\frac{d^\alpha}{dt^\alpha} f(t) = \frac{1}{\Gamma(1 - \alpha)} \int_0^t f'(t - y) y^{-\alpha} \, dy \qquad (5)$$

which is very useful for fractional time derivatives. Noting that the integral (5) is a convolution we can write

$$\frac{d^\alpha f(t)}{dt^\alpha} = \frac{df(t)}{dt} \star \frac{t^{-\alpha}}{\Gamma(1 - \alpha)} \qquad (6)$$

which relates the fractional derivative to a power law memory function.

2.3. Transforms of Fractional Derivatives

[11]　For partial differential equations, it is useful to use Fourier transforms in space and Laplace transforms in time. Since the transform of a power law is another power law, it is easy to check using (4) and (6) the Fourier and Laplace transforms pairs:

$$\frac{d^\alpha f(x)}{dx^\alpha} \leftrightarrow (ik)^\alpha \hat{f}(k)$$

$$\frac{d^\gamma f(t)}{dt^\gamma} \leftrightarrow s^\gamma \tilde{f}(s) - s^{\gamma-1} f(0) \qquad (7)$$

using $t^{-\gamma}/\Gamma(1 - \gamma) \leftrightarrow s^{\gamma-1}$.

2.4. Examples of Fractional Derivatives

[12]　Use the Laplace transform pair $t^{-\gamma}/\Gamma(1 - \gamma) \leftrightarrow s^{\gamma-1}$ along with the Laplace transform (7) to check that the α-order fractional derivative of t^p is $t^{p-\alpha}\Gamma(p+1)/\Gamma(p+1-\alpha)$ which reduces to the usual form when α is an integer. The Fourier transform (7) can be used to show that the α-order fractional derivative of $\sin x$ is $\sin(x + \pi\alpha/2)$, which reduces to the usual formula for integer α using standard trigonometric identities.

The α-order fractional derivative of e^{bx} is $b^\alpha e^{bx}$ and so forth. The point is that fractional derivatives are natural analogues of their integer-order cousins.

3. Classical Random Walk, Central Limit Theorem, and the ADE

[13]　Sediment transport has long been modeled as a stochastic sequence of hops and rest periods [*Einstein*, 1937; *Sayre and Hubbell*, 1965] leading to emergent properties after long time. It is also common to represent Earth surface transport process using diffusion-type models arising from the combination of a continuity equation with transport (flux) laws (since *Culling* [1960]). Random walk and diffusion models are related. Specifically, diffusion equations govern the stochastic processes that arise when the scaling limit of random walk is taken. Here we describe the type of particle motion that may be well modeled by a classical ADE so that the exact nature of our fractional generalizations will be clear. We can approach the advection-dispersion equation from either a Lagrangian or Eulerian point of view. By using a Lagrangian (following the progress of an individual particle with time) approach, the exact nature of the transport process is clarified.

3.1. Lagrangian Approach to the ADE

[14]　Our goal is to describe the motion of an ensemble of particles as measured by its concentration (or mass) in space and time $C(x, t)$. The distribution of particles within the plume will be represented by the pdf governing the location of a single particle in space. The discrete stochastic model we choose to develop this distribution is the random walk. We write the random particle location $X(t)$ as sum of stationary random jump lengths Y_i separated by time steps of length Δt:

$$X(t) = \sum_{n=1}^{t/\Delta t} Y_n.$$

Then we can use the Central Limit Theorem (CLT) to estimate the distribution of $X(t)$ at long time. The law of large numbers (LLN) says that the average of independent and identically distributed (IID) random variables with mean μ converges to the theoretical average:

$$\frac{Y_1 + \cdots + Y_n}{n} - \mu \to 0 \qquad (8)$$

as n becomes large. The CLT refines this statement by approximating the deviation between these two terms. It says that when appropriately rescaled, the sum of IID random variables with mean μ and standard deviation σ converges to a standard normal distribution:

$$\frac{Y_1 + \cdots + Y_n - n\mu}{\sigma n^{1/2}} \to N(0, 1).$$

We use this theorem to approximate the sum of IID particle jumps

$$Y_1 + \cdots + Y_n \approx n\mu + \sigma n^{1/2} N(0, 1). \qquad (9)$$
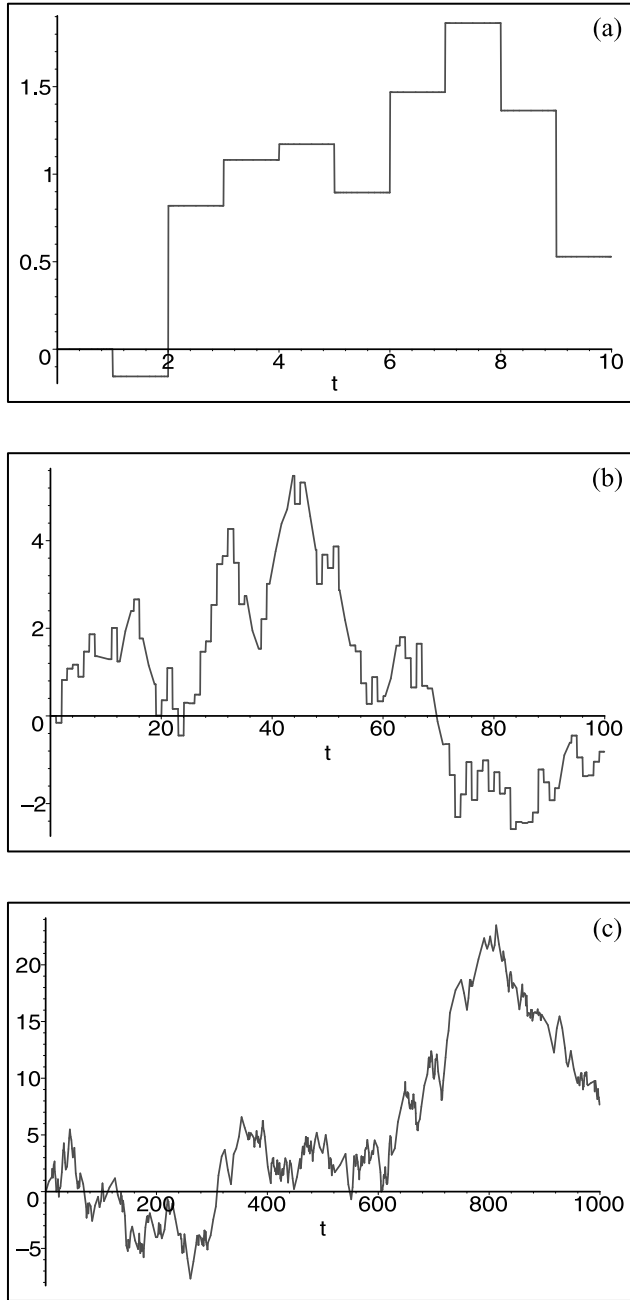
that governs particle location after a number of jumps. The right-hand side of (10) is called Brownian motion with drift. It combines a deterministic advective drift with a stochastic diffusion term $Z(t) = (2Dt)^{1/2}N(0, 1)$ that spreads like $t^{1/2}$ (Fickian scaling). The ADE solution $C(x, t)$ given by (11) is the probability density of the process $vt + Z(t)$ that represents the location of a randomly selected particle at time $t > 0$, assuming that particle location $x = 0$ at the initial time $t = 0$. Figure 2a illustrates the simple random walk. Figure 2b shows the same random walk at a longer time scale. Figure 2c shows the Brownian motion that emerges as the long-time scaling limit of this simple random walk. The continuous graph of the particle path is a random (not generated from a deterministic pattern) fractal with Hausdorff dimension 3/2 [*Mandelbrot*, 1982]. The abrupt jumps seen in the random walk disappear in the scaling limit. Figure 3 illustrates the probability density $C(x, t)$ of particle locations for the Brownian motion limit process.

3.2. Eulerian Approach to the ADE

[15] Using an Eulerian approach, we choose a specific location in space and describe particle motion through that location with time. From this perspective, we begin with a conservation of particle mass equation that equates the rate of mass change at a location with the difference between the mass of particles entering and leaving:

$$n\frac{\partial C(x,t)}{\partial t} = -\frac{\partial F(x,t)}{\partial x}, \tag{12}$$

where effective porosity $n = 1$ for transport at the surface, particle concentration C is in mass per volume, and flux F in mass per area per time. If particle flux is assumed to be by advection and Fickian dispersion:

$$F = vnC - n\mathcal{D}\frac{\partial C}{\partial x}, \tag{13}$$

where v is average particle velocity and $\mathcal{D}$ is a dispersion coefficient, then we obtain the advection-dispersion equation (also known as the Fokker Planck equation [*Feller*, 1971]):

$$\frac{\partial C(x,t)}{\partial t} = -v\frac{\partial C}{\partial x} + \mathcal{D}\frac{\partial^2 C(x,t)}{\partial x}. \tag{14}$$

[16] The solution to the ADE can be obtained using Fourier transforms:

$$\frac{\partial \hat{C}(k,t)}{\partial t} = -v(ik)\hat{C}(k,t) + \mathcal{D}(ik)^2\hat{C}(k,t). \tag{15}$$

Solve for C and use initial conditions $C(x, 0) = \delta(0)$ to find

$$\hat{C}(k,t) = e^{\left(-vt(ik)+Dt(ik)^2\right)} \tag{16}$$

the Fourier transform of a Gaussian density (11) with mean $\mu = vt$ and variance $\sigma^2 = 2\mathcal{D}t$.

[17] It is interesting that the deterministic solution to a partial differential equation should be a pdf. This important observation means that random behavior exhibits a deter-
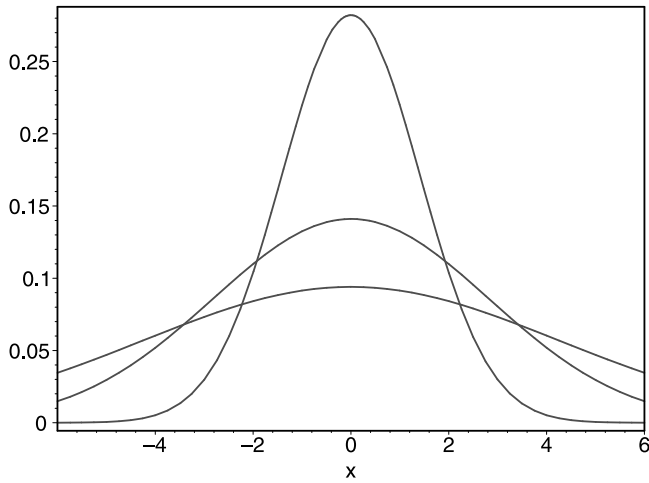
Figure 2. Comparison of random walk traces at increasing time scale and in the scaling limit as a Brownian motion. (a) A simple random walk $X(t)$ simulates particle motion. (b) Simple random walk $X(t)$ at a longer time scale. (c) Brownian motion as the scaling limit of a random walk $X(t)$. Particle graph is a random fractal with dimension 3/2.

Let the number of jumps be the total time divided by time per jump $n = \frac{t}{\Delta t}$ and recast the CLT to suit the random sum

$$Y_1 + \cdots + Y_n \approx t\frac{\mu}{\Delta t} + \frac{\sigma}{\sqrt{\Delta t}}t^{1/2}N(0,1). \tag{10}$$

Let $v = \frac{\mu}{\Delta t}$ and $D = \frac{\sigma^2}{2\Delta t}$ and we find a Gaussian density

$$C(x,t) = \frac{1}{\sqrt{2\pi \cdot 2\mathcal{D}t}}e^{-\frac{(x-vt)^2}{2\cdot 2\mathcal{D}t}} \tag{11}$$

Figure 3. Brownian motion density function $C(x, t)$ describing particle spreading away from plume center of mass at time $t = 1, 4$, and 9 in the scaling limit. Note the square root spreading rate and fast tail decay.

ministic regularity at long time. The location $vt + Z(t)$ of a randomly selected particle is unknown, but even so, the relative concentration of particles is predictable. We obtain the same solution using the Eulerian perspective of Fickian particle jumps and conservation of solute mass, or the Lagrangian random walk formulation taken to its scaling limit by applying the CLT. The assumptions underlying the CLT must hold for a Gaussian limit to emerge. This means that there are assumptions buried in Fickian/mass conserving ADE that must hold for it to be applicable. Our focus here is that, in order for the ADE to emerge, there can be only moderate deviation from the average jump size. Since it is well known that the ADE and its solutions do not always reproduce essential features of sediment or solute transport (e.g., *Benson* [1998], *Gooseff et al.* [2003], *Wörman et al.* [2007], *Neuman and Tartakovsky* [2009], and E. Foufoula-Georgiou et al. (Normal and anomalous dispersion of gravel tracer particles in rivers, submitted to *Journal of Geophysical Research*, 2009a), as well as references in this special issue on stochastic transport and emergent scaling at the Earth surface), we will now consider models that allow less stringent assumptions. We will also explore the long memory case where a time component is introduced by allowing random waiting times between jumps. In sections 4 and 5, we introduce fractional-in-space ADEs caused by heavy-tailed velocity distributions, and fractional-in-time ADEs caused by heavy-tailed residence times.

3.3. Characteristics of ADE Solutions

[18] If tracer transport is well modeled by a classical ADE, then long-term transport characteristics (of a pulse of tracer) will resemble the Green's function (point source) solutions [*Arfken and Weber*, 1995] to traditional integer-order advection-dispersion equations (Figure 4). These characteristics include the following.

[19] 1. The spatial snapshot characteristics are Gaussian (symmetric bell-shaped) concentration profiles, plume edges that decay rapidly, snapshot width that spreads like $t^{1/2}$, and total mass that remains constant over time.

[20] 2. The characteristics of the flux at position x are bell-shaped breakthrough curves, leading and trailing edges that decay rapidly, breakthrough curve width that grows like $x^{1/2}$, and area under breakthrough curve that remains constant.

4. Fractional-in-Space ADEs

[21] A variety of field and theoretical studies suggest superdiffusive nonlocality in transport of tracers at the Earth surface. For example, reanalysis of tracer studies in sand and gravel bed streams revealed hop length distributions with heavy tails [*Bradley et al.*, 2009]. E. Foufoula-Georgiou et al. (A non-local theory for sediment transport on hillslopes, submitted to *Journal of Geophysical Research*, 2009b) argue that transport on hillslopes is nonlocal and that sediment flux must be calculated using not just the local gradient, but also that of upslope topography. *Stark et al.* [2009] use a fractionally integrated flux term to capture nonlocal effects in a model of bedrock channel evolution that includes the effect of hillslope sediment production on channel bed sediment buffering and bedrock erosion. These studies all suggest fractional flux terms to represent nonlocality in transport.

[22] K. M. Hill et al. (Particle size dependence of the probability distribution functions of travel distances of gravel particles in bed load transport, submitted to *Journal of Geophysical Research*, 2009) suggest the source of power law hop lengths in bed load transport. They present and review experimental data to justify an exponential step length for particles of a given size. Since mean step length varies with particle size, the overall step length for all particles is a mixture of those exponential distributions. Using standard models (e.g., Gamma distribution) for the pdf of grain size leads to an overall step length pdf with a heavy power law tail. Even though neither the grain size distribution nor the
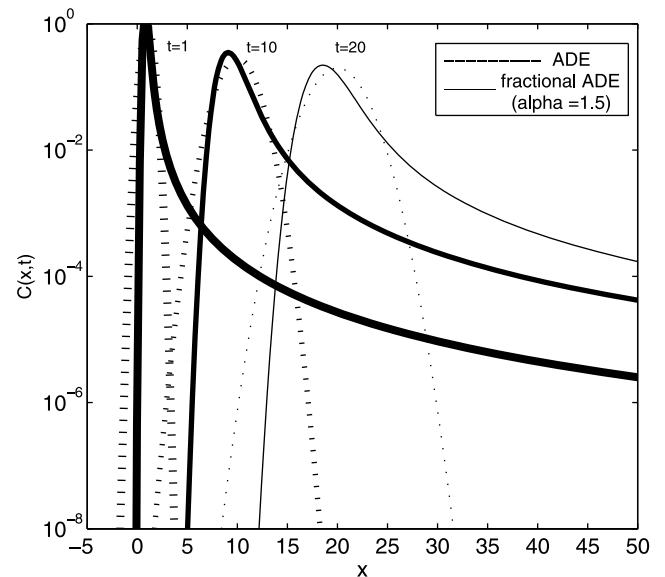

Figure 4. Comparison of the solutions in space to integer-order and fractional ADEs at time $t = 1$, $t = 10$, and $t = 20$. For both models, $v = 1$ and $D = 0.1$. The heavy leading edges of the α-stable solutions to the fractional ADE decay as $C(x) \approx x^{-\alpha-1}$.

step length pdf for grains of a given diameter are heavy tailed, the mixture distribution turns out to have a heavy tail. This result shows that a fractional Exner equation (Foufoula-Georgiou et al., submitted manuscript, 2009a) is applicable to bed load transport. It also highlights the need for additional experiments and analysis to improve estimates of grain size distribution, step length for moving particles, as well as entrainment rate for particles of varying size. Here we develop space fractional ADEs used to model superdiffusive transport using both the Lagrangian (particle tracking) and Eulerian (conservation of mass) approach.

4.1. Lagrangian Approach to Fractional-in-Space ADEs

[23] If the density of jump lengths Y_i is the heavy-tailed density $p(x)$, then the integral $\sigma^2 = \int_{-\infty}^{\infty} (X_i - \mu)^2 p(x) dx$ diverges. Then the classical CLT we use to determine the density of the sum of jump lengths $X(t)$ does not hold. A more general form of the CLT exists, however, and says that the properly rescaled sum of stationary IID random variables with even infinite variance converges in distribution to an α-stable density, denoted S_α, with mean μ, spread σ, tail parameter α, and skewness β [Feller, 1971; Gnedenko and Kolmogorov, 1968]. Here we assume that particle jumps are heavy tailed in the direction of flow only.

$$\frac{Y_1 + \cdots + Y_n - n\mu}{\sigma n^{1/\alpha}} \to S_\alpha(\mu = 0, \sigma = 1, \alpha, \beta = 1). \quad (17)$$

Note that the Gaussian distribution is α stable with $\alpha = 2$ (in which case the skewness is irrelevant), making this CLT a true generalization of the classical version.

[24] As before, recast the generalized CLT (17) to approximate the sum of random jumps:

$$\begin{aligned} Y_1 + \cdots + Y_n &\approx n\mu + \sigma n^{1/\alpha} S_\alpha(0, 1, \alpha, \beta) \\ Y_1 + \cdots + Y_n &\approx t\frac{\mu}{\Delta t} + \frac{\sigma}{\Delta t^{1/\alpha}} t^{1/\alpha} S_\alpha(0, 1, \alpha, \beta) \end{aligned} \quad (18)$$

and let $v = \frac{\mu}{\Delta t}$ and $\mathcal{D} = \frac{\sigma^\alpha}{\Delta t}$ to find an α-stable density

$$\hat{C}(k,t) = e^{(-vt(ik) + \mathcal{D}t(ik)^\alpha)}$$

in Fourier space. The α-stable density cannot be written in closed form in real space. A variety of methods exist to estimate the inverse transform numerically [Nolan, 1998].

[25] Figure 5a illustrates a simple random walk with heavy-tailed particle jumps. Figure 5b shows the same random walk at a longer time scale. Figure 5c shows the stable Lévy motion that emerges as the long-time scaling limit of this heavy-tailed random walk. The graph of the particle path is a random fractal with dimension $2 - 1/\alpha$. The large jumps seen in the random walk persist in the scaling limit. Figure 6 illustrates the probability density $C(x, t)$ of particle locations for the stable Lévy motion limit process. This particle motion process exhibits a superdiffusive spreading rate, skewness, and power law right tail (early arrivals downstream).

[26] The right-hand side of (18) is called α-stable Lévy motion with drift. This limit process $vt + Z(t)$ represents the location of a randomly selected particle at time $t > 0$, as-

suming that particle location $x = 0$ at the initial time $t = 0$. The diffusion term $Z(t) = t^{1/\alpha} S_\alpha (0, 1, \alpha, \beta)$ exhibits non-Fickian scaling, a characteristic often seen in laboratory and field studies [Benson et al., 2000a, 2000b, 2001]. Since $\alpha < 2$ the scaling factor $t^{1/\alpha}$ grows faster (the plume spreads faster) than the classical ADE case $\alpha = 2$, so this model is often called superdiffusive. Aside from its super-Fickian scaling, Lévy motion has other features that distinguish it from its close cousin, Brownian motion. Lévy motion probability densities are positively skewed, with a long leading tail [Samorodnitsky and Taqqu, 1994]. In fact, the probability mass a distance r units or more from the plume center of mass falls off like $x^{-\alpha}$ so that particles are much more likely to race ahead of the mean.

4.2. Eulerian Approach to Fractional-in-Space ADEs

[27] The Eulerian approach accounts for bulk mass movements into and out of a finite size control volume of edge size $\Delta x = h$ during a short time step Δt, as in Figure 7. In a fractal porous medium (and perhaps, in a fractal river network), the velocity of different particles in the control volume can vary widely, so that a particle can enter the control volume from long distances upstream via high-velocity paths. The fractal medium imposes a power law velocity distribution, leading to a fractional Fick's Law $F = -\mathcal{D}\partial^{\alpha-1}C/\partial x^{\alpha-1}$ for dispersive flux [Schumer et al., 2001], since dispersion comes from variations in velocity. The Grunwald weights in Figure 1 code the velocity distribution. A fractional dispersive flux in the solute mass conservation equation (12) leads to a fractional-in-space ADE

$$\frac{\partial C(x,t)}{\partial t} = -v\frac{\partial C(x,t)}{\partial x} + \mathcal{D}\frac{\partial^\alpha C(x,t)}{\partial x^\alpha}. \quad (19)$$

Use Fourier transforms to solve the space fADE (19):

$$\begin{aligned} \frac{\partial \hat{C}(k,t)}{\partial t} &= -v(ik)\hat{C}(k,t) + \mathcal{D}(ik)^\alpha \hat{C}(k,t) \\ \hat{C}(k,t) &= \exp\left[-vt(ik) + \mathcal{D}t(ik)^\alpha\right] \end{aligned}$$

which is the Fourier transform of an α-stable density with shift $\mu = vt$, spread $\sigma^\alpha = \mathcal{D}t$, skewness $\beta = 1$, and tail parameter $1 < \alpha \leq 2$. More extreme deviations from the mean velocity are represented by heavier-tailed jump distributions and, in turn, are governed by fractional ADEs with smaller order fractional derivatives on the flux term [Clarke et al., 2005].

[28] An alternative Eulerian derivation of the space fADE uses a fractional conservation of mass with a traditional Fickian flux [Meerschaert et al., 2006]. Foufoula-Georgiou et al. (submitted manuscript, 2009a) develop a probabilistic Exner equation for sediment transport, which is applicable when particle step lengths follow a heavy-tailed (power law) pdf. This asymptotic governing equation for the movement of entrained particles is valid at scales long enough to encompass many particle jumps. Using an active layer approach, neglecting porosity, and assuming equilibrium (steady, uniform) bed load transport of grains of uniform size over a bed, the probabilistic Exner equation in the presence of a heavy-tailed step length is $\frac{L_a}{E}\frac{\partial f_a}{\partial t} = -v\frac{\partial f_a}{\partial x} + D\frac{\partial^\alpha f_a}{\partial x^\alpha}$, where

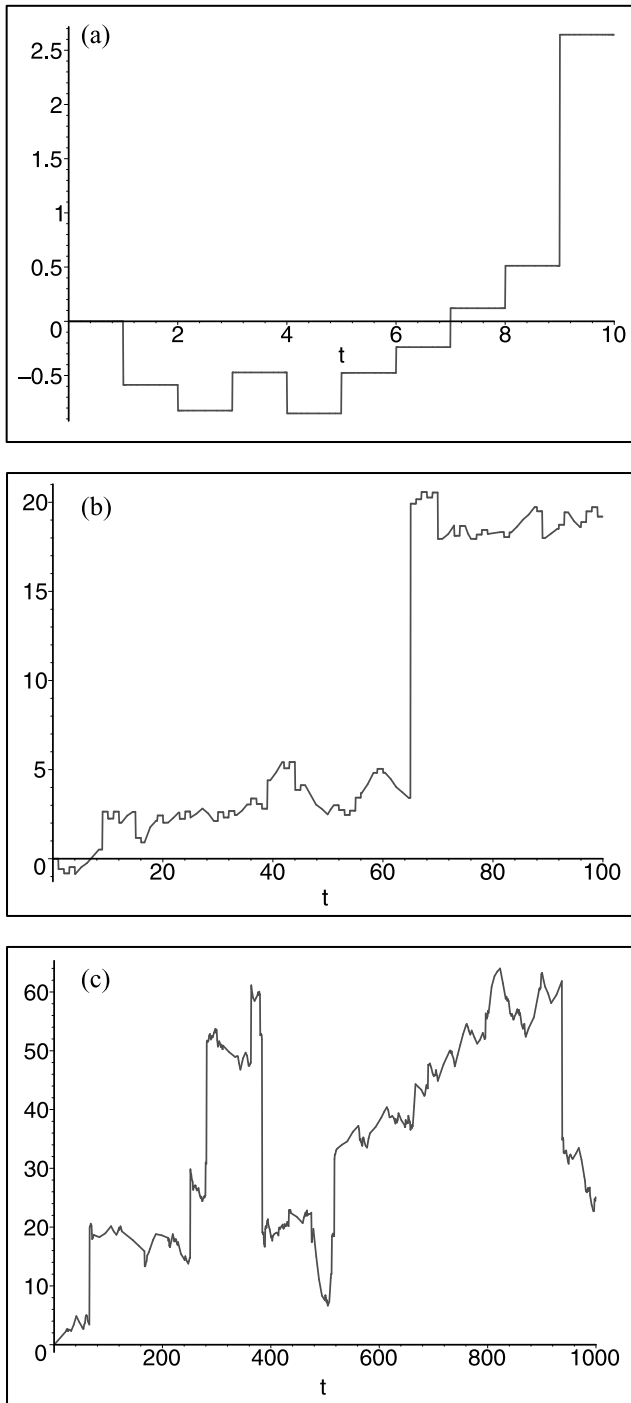**Figure 6.** Lévy motion density function $C(x, t)$ describing particle spreading away from plume center of mass at time $t = 1$, 4, and 9 in the scaling limit. Note the superdiffusive spreading rate, skewness, and power law tail.

4.3. Characteristics of Space fADE Solutions

[29] Characteristics of the Green's function solutions to the advection-dispersion equation with a fractional-order term in space (Figure 4) are as follows.

[30] 1. The spatial snapshot characteristics are α-stable concentration profiles skewed with long right tail, plume leading edges that decay like a power law $x^{-\alpha-1}$, snapshot width that spreads like $t^{1/\alpha}$, and total mass that remains constant over time.

[31] 2. The characteristics of the flux at position x are asymmetric breakthrough curves, long leading edge, breakthrough curve width that grows like $x^{1/\alpha}$, and area under breakthrough curve that remains constant.

5. Fractional-in-Time ADEs

[32] Tracer particles at the Earth surface spend more time at rest than in motion [*Sadler*, 1981; *Leopold et al.*, 1964; *Tipper*, 1983]. For example, frequency distributions of bed load path length are positively skewed, indicating that many particles do not move from the point of tracer input over the measurement period [*Hassan and Church*, 1992; *Pryce and Ashmore*, 2003]. Small deviations in waiting times will not affect long-term dispersion rates, but heavy-tailed waiting times will. This affects overall bed load rates [*Singh et al.*,

Figure 5. Comparison of heavy-tailed random walk traces at increasing time scale and in the scaling limit as a stable Lévy motion. (a) A heavy-tailed random walk $X(t)$ simulates anomalous particle motion. (b) Heavy-tailed random walk $X(t)$ at a longer time scale. (c) Stable Lévy motion as the scaling limit of a random walk $X(t)$. Particle graph is a random fractal with heavy-tailed jumps.

f_a is the fraction of tracer particles in the active layer, v, D are as in the space fADE (19), L_a is the thickness of the active layer, and E is the entrainment rate. Dividing both sides by L_a/E yields an equation mathematically identical to the space fADE (19), so that the same solution methods apply.
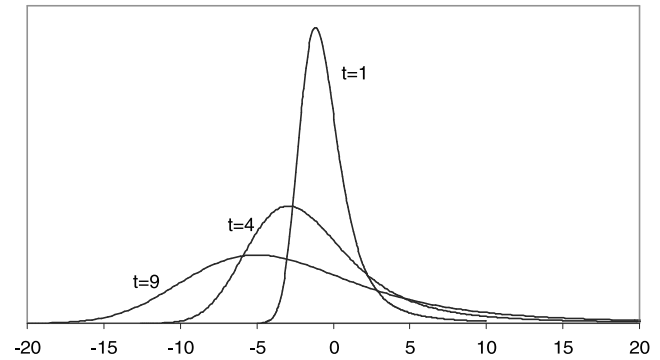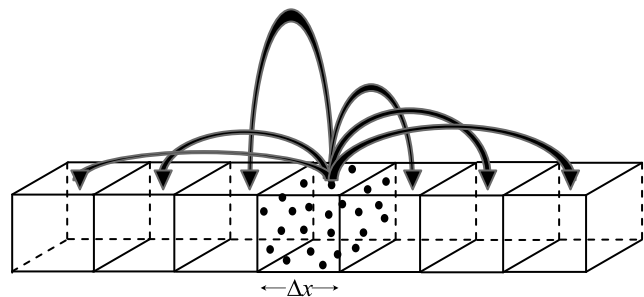

Figure 7. When governed by a fractional-in-space ADE, particle hop length during a small time step Δt may be much larger than the mean size. In finite difference implementations for fractional ADEs, probability of particle hop length decays as a power law with distance [after *Schumer et al.*, 2001].

2009] and the resulting transport characteristics can be accommodated by time-fractional ADE, which will be developed from both the Lagrangian and Eulerian view. Evidence for heavy-tailed waiting times in transport is captured in the depositional record [*Schumer and Jerolmack*, 2009]. A promising avenue for future research is to examine waiting times between entrainment events, to determine whether a time-fractional Exner equation may be useful to incorporate particles outside the active layer, including deeply buried particles, those incorporated into the hyporheic zone, and particles outside the normal flow path of a river (sandbars, floodplain) (e.g., see discussion by Foufoula-Georgiou et al. (submitted manuscript, 2009a)).

5.1. Lagrangian Approach to Fractional-in-Time ADEs

[33] A continuous time random walk (CTRW) imposes a random waiting time J_n before the particle jump Y_n occurs. The particle location at time t is

$$X(t) = Y_1 + \cdots + Y_n,$$

where $n = N(t)$ is the number of jumps by time t. Suppose the particle jumps have mean zero so that the centered (generalized) CLT applies:

$$Y_1 + \cdots + Y_n \approx n^{1/\alpha} Z,$$

where Z is stable (normal if $\alpha = 2$). The sum $J_1 + \cdots + J_n$ gives the time of the n*th* particle jump. If the waiting times have a finite mean ν then the law of large numbers (8) shows that the nth jumps happens at time $t = T_n \approx n\nu$ and then $X(t) \approx Y_1 + \cdots + Y_{t/\nu}$ leads to the classical ADE. On the other hand, if the waiting times J_n are heavy tailed with power law index $0 < \gamma < 1$ and scale $\sigma = 1$ then the generalized CLT yields

$$\frac{J_1 + \cdots + J_n - n\nu}{n^{1/\gamma}} \to W, \tag{20}$$

where W is distributed like $S_\gamma(\mu = 0, \sigma = 1, \gamma, \beta = 1)$. Since $\gamma < 1$, we find $n\nu/n^{1/\gamma} \to 0$, and so the centering term in (20) can be neglected. Then the nth jump occurs at time

$$t = J_1 + \cdots + J_n \approx n^{1/\gamma} W \tag{21}$$

for large n. Solving for n shows that the particle location $X(t) = Y_1 + \cdots + Y_n \approx n^{1/\alpha} Z$ where $n \approx (t/W)^\gamma$ for large n. Putting this all together, we see that

$$X(t) \approx (t/W)^{\gamma/\alpha} Z$$

and this approximation is exact in the scaling limit, where the number of jumps tends to infinity [*Meerschaert and Scheffler*, 2004]. If $g(t)$ is the pdf of W, a change of variables [*Meerschaert and Scheffler*, 2004] shows that $u = (t/W)^\gamma$ has pdf

$$q(u, t) = \frac{t}{\gamma} u^{-1-1/\gamma} g(tu^{-1/\gamma})$$

for $u > 0$. If $f(x, u)$ is the pdf of $u^{1/\alpha} Z$ then taking a weighted average with respect to u [*Meerschaert and Scheffler*, 2004] shows that the limit particle location x at time t has pdf

$$C(x, t) = \int_0^\infty f(x, u) q(u, t)\, du \tag{22}$$

a scale mixture of stable densities. Since

$$\begin{aligned} \hat{f}(k, u) &= e^{\mathcal{D}u(ik)^\alpha} \\ \tilde{q}(u, t) &= s^{\gamma-1} e^{-us^\gamma} \end{aligned} \tag{23}$$

(for the Laplace transform formula, see *Meerschaert et al.* [2002b]) a simple integration shows that the Fourier-Laplace transform of $C(x, t)$ is

$$\overline{C}(k, s) = \frac{s^{\gamma-1}}{s^\gamma - \mathcal{D}(ik)^\alpha}$$

which will lead to the space-time fractional ADE. Rearrange to get $s^\gamma \overline{C}(k, s) - s^{\gamma-1} = \mathcal{D}(ik)^\alpha \overline{C}(k, s)$ and invert the Laplace and Fourier transforms using (7) to get

$$\frac{\partial^\gamma C(x, t)}{\partial t^\gamma} = \mathcal{D}\frac{\partial^\alpha C(x, t)}{\partial x^\alpha}$$

using the Caputo derivative in time, where the point source initial condition implies $\hat{C}(k, t = 0) = 1$. Adding an advective drift yields the space-time fractional ADE

$$\frac{\partial^\gamma C(x, t)}{\partial t^\gamma} = -v\frac{\partial C(x, t)}{\partial x} + \mathcal{D}\frac{\partial^\alpha C(x, t)}{\partial x^\alpha} \tag{24}$$

which governs the CTRW particle density in the long-time limit. It is important to note that the parameter α codes the large particle jumps (early arrivals) and γ controls the long waiting times (residence times). A more detailed analysis using the CLT leads to higher-order temporal derivatives [*Baeumer et al.*, 2005; *Baeumer and Meerschaert*, 2007].

[34] The limit process $X(t) = Z(T(t))$ is a subordinated Lévy (or Brownian) motion. The outer process is the random walk limit discussed previously. The inner process $T(t) = (t/W)\gamma$ adjusts for the time a randomly selected particle spends in motion (e.g., see recent work by *Ganti et al.* [2009] who propose a subordinated Brownian motion model for sediment transport). We call $u = T(t)$ the operational time, since it counts the number of particle jumps by time t. Since the operational time process incorporates memory effects, it is non-Markovian, and it is simpler to understand its inverse process $t = W(u)$ that maps operational time back to clock time t. The process $W(u) = u^{1/\gamma} W$ comes from (21) and it is another Lévy motion with index $\gamma < 1$. Then the operational time process $u = T(t)$ is the inverse of this Lévy process. The scaling $W(u) = u^{1/\gamma} W$ is consistent with the inverse scaling $T(t) = t^\gamma T$ already noted. The scaling $X(t) = Z(T(t)) = Z(t^\gamma T) = t^{\gamma/\alpha} Z(T) = t^{\gamma/\alpha} X$ shows that particles following the space-time fractional ADE spread at rate $t^{\gamma/\alpha}$ which is slower than the ADE if $\alpha = 2$. This model is often called subdiffusive. The random time change T has finite
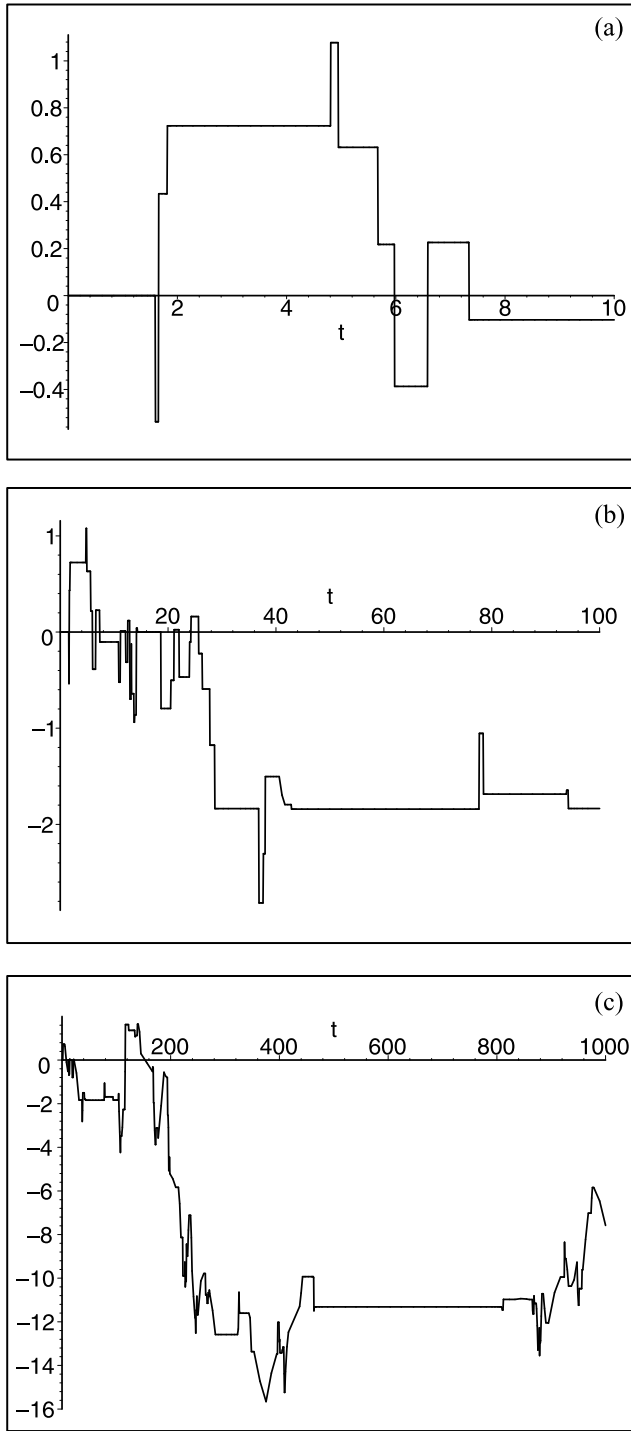
Figure 8. Comparison of heavy-tailed waiting time CTRW traces at increasing time scale and in the scaling limit as a subordinated Brownian motion. (a) CTRW with heavy-tailed waiting times simulates subdiffusive particle motion. (b) CTRW at a longer time scale. (c) Subordinated Brownian motion as the CTRW scaling limit. Long resting times persist in the limit process.

moments of all orders, so in the heavy-tailed case $\alpha < 2$ it does not affect the tails of $X(t)$ which still fall off like $x^{-\alpha}$ [Meerschaert and Scheffler, 2004]. The mixture integral (22) is a weighted average of the PDF $f(x, u)$ of the random

walk limit $Z(u)$ according to the PDF $q(u, t)$ of the inverse Lévy process $T(t)$.

[35] Figure 8a illustrates a CTRW with heavy-tailed waiting times. Figure 8b shows the same CTRW at a longer time scale. Figure 8c shows the continuous particle path of the subordinated Brownian motion that emerges as the long-time scaling limit of this CTRW. The long resting times (particle retention) seen in the CTRW persist in the scaling limit.

5.2. Eulerian Approach to Fractional-in-Time ADEs

[36] The Eulerian approach accounts for bulk mass movements into and out of a control volume of edge size $\Delta x = h$ during a short time step Δt, as in Figure 7. The time fADE includes memory effects, allowing particle residence times for long periods. This means that particles can enter the control volume at the current time step from locations upstream in time as depicted in Figure 9. A power law memory function [Haggerty and Gorelick, 1995; Haggerty et al., 2000, 2002] implies that the time flux can be coded using a discrete convolution in time $\Sigma C(x, t - jh)w_j$ using the power law Grunwald weights from Figure 1. This leads to a time-fractional analogue $n\partial^\gamma C(x, t)/\partial t^\gamma = -\partial(x, t)/\partial x$ to the conservation of solute mass equation (12) that combines with the usual advective and dispersive flux equation (13) to produce the time fADE

$$\frac{\partial^\gamma C(x,t)}{\partial t^\gamma} = -v\frac{\partial C(x,t)}{\partial x} + \mathcal{D}\frac{\partial^2 C(x,t)}{\partial x^2}. \qquad (25)$$

If power law residence time (memory function) is combined with power law velocity distribution, we recover the same space-time fADE (24) derived from the Lagrangian model. The time-fractional parameter γ codes retention, since it implies that the memory function $t^{-\gamma}$ is a power law, and so it can be estimated from the late-time tail of the breakthrough curve [Schumer et al., 2003].

[37] The solution $C(x, t)$ to the time fADE (25) is the probability density of the subordinated process $X(t) = Z(T(t))$ that models the location of a randomly selected particle. The solution formula (22) mixes the density of $Z(u)$ according to the operational time process $u = T(t)$. The outer process $Z(u)$ is a Brownian motion connected with the right-hand side of (25), and the inner process compensates for the memory effects of the fractional time derivative on the left-hand side of (25).

5.3. Characteristics of Time (and Space) fADE Solutions

[38] Characteristics of the Green's function solutions to the advection-dispersion equation with a fractional-order term in time and possibly space are as follows.

[39] 1. The spatial snapshot characteristics are subordinated α-stable concentration profiles skewed with long right tail if $\alpha < 2$, plume leading edges that decay like a power law $x^{-\alpha-1}$ if $\alpha < 2$, snapshot width that spreads like $t^{\gamma/\alpha}$, and total mass that remains constant over time.

[40] 2. The characteristics of the flux at position x are breakthrough curve tail that decays as $t^{-\gamma-1}$; breakthrough curve width that grows like $x^{\gamma/\alpha}$; if $\alpha < 2$, immediate spike in flux then strong leading edge; and area under breakthrough curve that is constant with time.
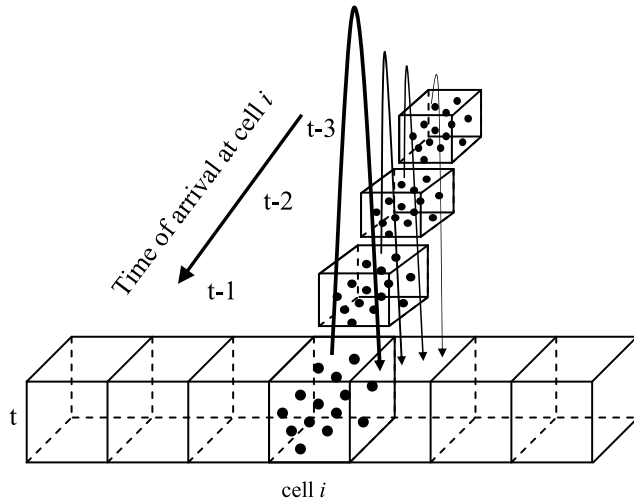
Figure 9. When governed by a fractional-in-time ADE, particles have memory of the time that they arrive at a given point. Their probability of release decays as a power law from arrival time.

5.4. Fractional ADEs for Mobile and Immobile Zones

[41] The fractional-in-time ADE describes the evolution of a tracer plume, but does not distinguish between particles moving at the Earth surface (with mobile concentration denoted C_m) and particles that have been immobilized (C_{im}), where $C = n_m C_m + n_{im} C_{im}$ [e.g., *Coats and Smith*, 1964], mobile porosity $n_m = 1$ at the surface and immobile porosity $n_i m$ may be less than 1 if availability of pore space is a control on immobilization of sediment or solute. This is significant because typical sampling methods for surface water and groundwater solute concentration permit only observation of mobile solute concentration. Mobile solute equations can predict absolute solute concentration rather than relative or normalized concentration C/C_0 because they account for mass loss to immobile zones with time [*Schumer et al.*, 2003].

[42] Traditional mobile-immobile equations assume that particles move between the mobile and immobile phases at an instantaneous rate proportional to the difference in concentration. If particles begin in an immobile phase, this implies that immobile concentration decays exponentially in time, as reflected in the late-time breakthrough curve. A multiple-rate mass transfer model (MRMT) uses a memory function to govern release from the immobile phase [*Haggerty and Gorelick*, 1995], and has been used to fit late time solute breakthrough curves in groundwater aquifers [*Haggerty et al.*, 2000]. Following *Schumer et al.* [2003] we write the MRMT equations for transport:

$$\frac{\partial C_m}{\partial t} + \beta \frac{\partial C_m}{\partial t} \star g(t) = LC_m - C_m(x, t = 0)\beta g(t)$$

$$\frac{\partial C_{im}}{\partial t} + \beta \frac{\partial C_{im}}{\partial t} \star g(t) = LC_{im} + C_m(x, t = 0)g(t), \tag{26}$$

where the capacity coefficient $\beta = n_{im}/n_m$, "$\star$" denotes convolution, $g(t)$ is the memory function, and we write $L =$

$-v\partial/\partial x + D\partial^2/\partial x^2$ for brevity. Equation (26) assumes that all solute begins in the mobile phase. If power law memory is of form $g(t) = t^{-\gamma}/\Gamma(1 - \gamma)$, the memory function convolution becomes the Caputo fractional derivative in time (6), and (26) becomes the fractal mobile-immobile equations

$$\begin{aligned}\frac{\partial C_m}{\partial t} + \beta \frac{\partial^\gamma C_m}{\partial t^\gamma} &= LC_m - C_{m,0}(x)\frac{\beta t^{-\gamma}}{\Gamma(1-\gamma)} \\ \frac{\partial C_{im}}{\partial t} + \beta \frac{\partial^\gamma C_{im}}{\partial t^\gamma} &= LC_{im} + C_{m,0}(x)\frac{t^{-\gamma}}{\Gamma(1-\gamma)}\end{aligned} \tag{27}$$

with $C_{m,0}(x) = C_m(x, t = 0)$ as in the work by *Schumer et al.* [2003]. Figure 10 shows the characteristic behavior of fractal mobile-immobile transport. The late-time behavior of the breakthrough curve is governed by the order of the time-fractional derivative. The key characteristics of the mobile zone fADE that differ from those of the fractional-in-time ADE are (1) total mass in the mobile zone decays with time as $\frac{t^{\gamma-1}}{\Gamma(\gamma)}$ and (2) if $\alpha < 2$, the breakthrough curve has a long leading edge but no immediate spike in flux.

6. Scaling Properties of Fractional ADEs

[43] The limiting stochastic process governed by any (traditional or fractional) ADE is self-similar and has useful scaling properties. For example, the traditional ADE governs Brownian motion with drift, so that relative concentration $C(x, t)$ in (11) gives the probability density for this stochastic process. There are actually two scales in this equation. The plume center of mass moves linearly, proportional to t, and the plume spreads more slowly, proportional to $t^{1/2}$ as t increases. To focus on the spread, adopt a moving coordinate system with origin at the plume center of mass. This converts to $v = 0$ in the ADE, so that it reduces to the diffusion/dispersion equation

$$\frac{\partial C(x,t)}{\partial t} = \mathcal{D}\frac{\partial^2 C(x,t)}{\partial x^2} \tag{28}$$

whose point source solution is

$$C(x,t) = \frac{1}{\sqrt{2\pi \cdot 2\mathcal{D}t}}e^{-\frac{x^2}{2 \cdot 2\mathcal{D}t}} \tag{29}$$

a mean zero normal density with variance $2\mathcal{D}t$. A snapshot graph of this density curve for any fixed t is bell shaped, centered at the origin, and as t increases, the snapshots are all the same shape. This scaling property is expressed mathematically as $C(x, t) = t^{-1/2}C(xt^{-1/2}, 1)$ which clearly shows that the concentration snapshot spreads away from its center of mass like $t^{1/2}$ and the plume peak concentration decreases at the same rate. This scaling is also evident in the Fourier transform $\hat{C}(k, t) = \exp[-\mathcal{D}tk^2]$ since evidently $\hat{C}(k, t) = \hat{C}(t^{1/2}k, 1)$. For the space fADE, the same moving coordinate system leads to $C(x, t) = t^{-1/\alpha}C(xt^{-1/\alpha}, 1)$ and again with $\hat{C}(k, t) = \exp[\mathcal{D}t(ik)^\alpha]$ we have $\hat{C}(k, t) = \hat{C}(t^{1/\alpha}k, 1)$. Thus the space fADE snapshot, a stable density with index α, spreads like $t^{1/\alpha}$ while its peak falls at the same rate. Solutions to the space-time fADE (24) with $v = 0$ can be expressed as $\hat{C}(k, t) = E_\gamma(t^\gamma \mathcal{D}(ik)^\alpha)$
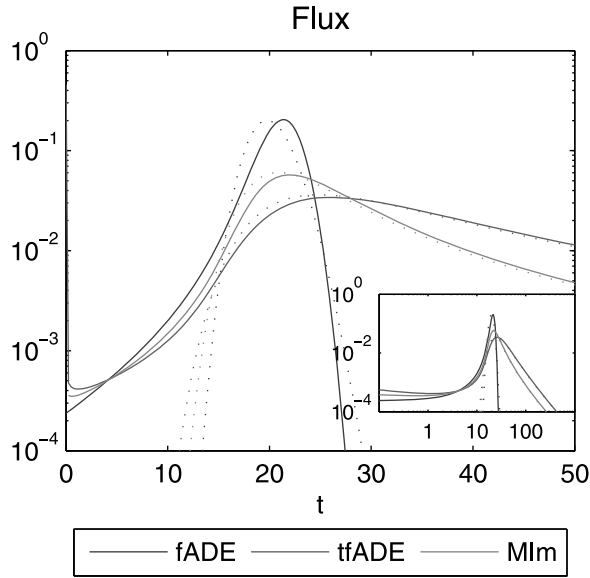
Flux

Figure 10. Flux at a distance of $x = 20$ versus time in semilog and log-log plots for solutions to equations (19), (24), and (26) with $v = 1$, $D = 0.1$, $\gamma = 0.8$, and $\beta = 1$ where applicable. Dotted lines represent the flux with $\alpha = 2$, and solid lines represent $\alpha = 1.5$.

[*Mainardi and Gorenflo*, 2000] where the Mittag-Leffler function

$$E_\gamma(z) = \sum_{k=0}^{\infty} \frac{z^k}{\Gamma(1 + \gamma k)}$$

is an extension of the exponential (the special case $\gamma = 1$) used in the theory of time-fractional equations. It is easy to see that $\hat{C}(k, t) = t^{\gamma/\alpha}\hat{C}(k, 1)$ and so the space-time fADE is also scale invariant after mean centering: The plume snapshot spreads like $t^{\gamma/\alpha}$ and the plume peak falls at the same rate [*Meerschaert et al.*, 2002a].

[44] If a transport model reveals scale dependence of parameters, it is likely that the model is scale-dependent, not the transport process itself. One option is to use a model with time-dependent parameters, but this is difficult to apply in practice. Using a model that includes the correct scaling is useful for prediction because its parameters will be constant in time. In the fractional-in-space and time case, the scaling rate $t^{\gamma/\alpha}$ can be obtained with nonunique $0 < \gamma \leq 1$ and $1 < \alpha \leq 2$ (for example, a scaling rate of $t^{0.56}$ can be obtained with $\alpha = 1.8$ and $\gamma = 1$ or $\alpha = 1.5$ and $\gamma = 0.83$). The tail properties of plume snapshots or breakthrough curves will be necessary to obtain the order of the space and time fractional derivatives. An analysis of plume moments may also be necessary for choosing the appropriate transport model [*Zhang et al.*, 2008]. The scaling rate for plumes following a mobile fractional ADE is [*Schumer et al.*, 2003] $C_m(x, t) = t^{\gamma - 1}t^{-\frac{\gamma}{\alpha}}C_m(t^{-\frac{\gamma}{\alpha}}x, 1)$. In summary, fADE plumes spread out from the center of mass according to precise scaling rates, that are determined by the order of the space or time derivative. A smaller index α on the space derivative implies faster (superdispersive) spreading, while a smaller γ

index on the time derivative yields a slower (subdispersive) spread. In practice, the superdispersive effect comes from high-velocity contrasts, while the subdiffusive behavior reflects long residence times.

7. CTRW Derivation of the Space-Time fADE

[45] The Lagrangian derivation of the space-time fADE is closely connected to the underlying CTRW model for particle transport [*Berkowitz et al.*, 2002, 2006]. Each random particle jump Y_n follows a random waiting time J_n. Suppose that Y_n has mean v and $P(Y_n - v > x) \approx x^{-\alpha}$ and $P(J_n > t) \approx t^{-\gamma}$ for large x and t. Then the jump pdf $p(x)$ of Y_n has Fourier transform $\hat{p}(k) = 1 - ikv + \mathcal{D}(ik)^\alpha + \cdots$ and the waiting time pdf $\psi(t)$ of J_n has Laplace transform $\tilde{\psi}(s) = 1 - s^\gamma + \cdots$ where we emphasize the dominant terms for small k and s. The master equation [*Montroll and Weiss*, 1965; *Scher and Lax*, 1973] (also used by *Furbish et al.* [2009a, 2009b] to describe probability of soil particle flux) gives the Fourier-Laplace transform of the CTRW particle density:

$$\overline{C}(k, s) = \frac{1 - \tilde{\psi}(s)}{s} \frac{1}{1 - \hat{p}(k)\tilde{\psi}(s)}. \qquad (30)$$

After substituting power law space and time jump pdf's into the master equation, we find

$$\overline{C}(k, s) \approx \frac{s^{\gamma - 1}}{s^\gamma + ikv - \mathcal{D}(ik)^\alpha} \qquad (31)$$

which rearranges to

$$s^\gamma\overline{C}(k, s) - s^{\gamma-1} = -ikv\overline{C}(k, s) + \mathcal{D}(ik)^\alpha\overline{C}(k, s).$$

Invert the Fourier and Laplace transforms to recover the space-time fADE (24). For light-tailed particle jumps, the Fourier transform $\hat{p}(k) = 1 - ikv + \mathcal{D}(ik)^2 + \cdots$ and the second derivative in space reappears. For light-tailed waiting times, the Laplace transform $\tilde{\psi}(s) = 1 - s + \cdots$ leading to the first derivative in time. The asymptotic approximation is identical to our earlier discussion, and it is only in the limit that the neglected terms vanish to produce the fADE (or the ADE). If the jump length and residence time densities are known exactly, it is possible to model transport with a discrete CTRW without taking the long time or scaling limit simply by using those densities in equation (30). In this case, a preergodic solution is reached that does not necessarily have scale invariance.

8. Relationship With Other Stochastic Models

[46] Fractional ADEs are related to other general stochastic process models of random particle motion. Here we give a brief discussion to provide context. The CTRW master equation (30) inverts to an integral equation for particle density $C(x, t)$ which is also known as the (generalized) master equation [*Klafter and Silbey*, 1980]. The convolution integral in this master equation can approximate fractional derivatives in space and/or time. The solution to this master equation gives the pdf of the CTRW particle density. The underlying particle motion process consists of space-time
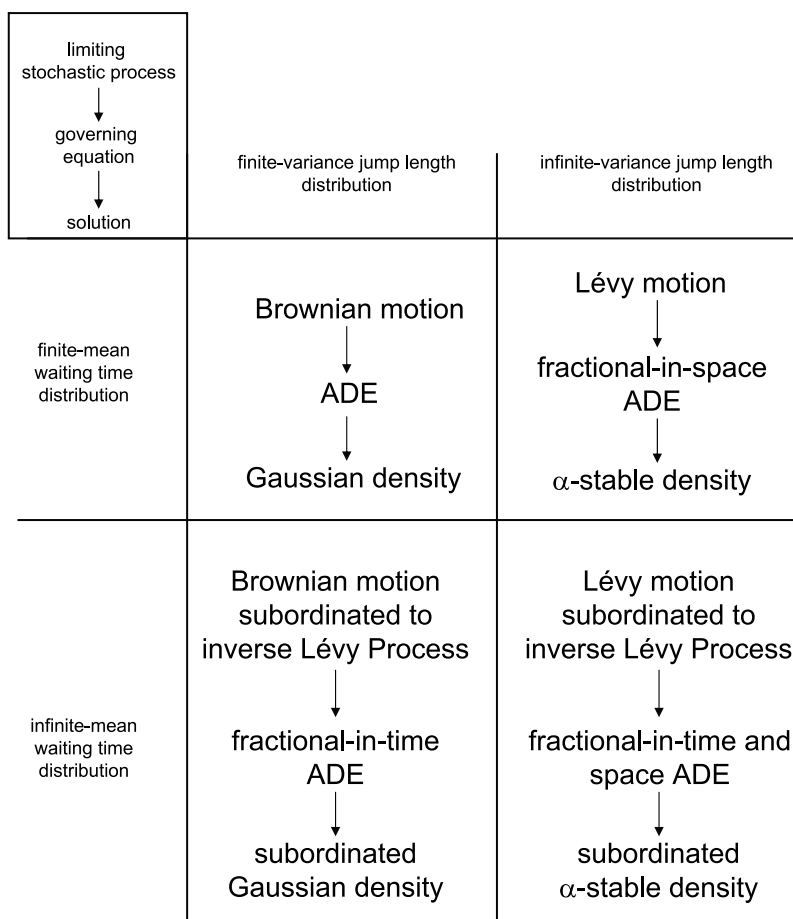
limiting stochastic process → governing equation → solution	finite-variance jump length distribution	infinite-variance jump length distribution
finite-mean waiting time distribution	Brownian motion ↓ ADE ↓ Gaussian density	Lévy motion ↓ fractional-in-space ADE ↓ α-stable density
infinite-mean waiting time distribution	Brownian motion subordinated to inverse Lévy Process ↓ fractional-in-time ADE ↓ subordinated Gaussian density	Lévy motion subordinated to inverse Lévy Process ↓ fractional-in-time and space ADE ↓ subordinated α-stable density

Figure 11. CTRW converges to different limiting stochastic process depending on the tail characteristics of the jump length distribution and waiting time distribution. Particles undergoing the limiting stochastic process are governed by ADEs with either integer-order or non-integer-order derivatives with solutions that are related to probability density functions. A CTRW with finite mean waiting time distribution converges in the scaling limit to the same stochastic process as the analogous random walk.

jumps as shown in Figures 2a, 5a, and 8a. Fractional advection-dispersion equations arise in the scaling limit. A different approach based on statistical mechanics leads to a continuously evolving stochastic model for particle motion, where particle flux is represented as a convolution integral [*Cushman*, 1997]. The space-time convolution can capture memory effects (time convolution) and nonlocal superdiffusive particle jumps (space convolution). The space-time fractional diffusion equation is a special case of this stochastic model, in which the convolution kernel is a power law [*Cushman and Ginn*, 1993, 2000]. A more complex but correspondingly general theory is reviewed by *Neuman and Tartakovsky* [2009]. That paper also compares and contrasts the various theories used in stochastic hydrology in more detail. The added generality allows a velocity field that varies in space and time [*Neuman*, 1990]. The variable coefficient fractional ADE represents the special case of a power law memory kernel in space and time. In any given situation, the practitioner will make an intelligent model selection that takes into account a trade-off between simplicity and generality. For example, it is possible to generate stochastic processes with nonstationary increments that have heavy

tails and satisfy classical ADEs with time-dependent dispersion tensors [*Berkowitz et al.*, 2002]. In our view, fractional advection dispersion equations represent the simplest model that incorporates the anomalous spreading and skewness often seen in transport at the Earth surface. They complement CTRW and other more detailed stochastic models with a simplified (limit) case appropriate for plume modeling at the large scale.

9. Summary: Use of Fractional ADEs in Modeling Earth Surface Transport

[47] Characterizing the collective behavior of particle transport on the Earth surface is a key ingredient for describing landscape evolution. Alternatives to local, diffusive transport laws are sought because these classical models do not always capture essential features of transport on hillslopes, valleys, river channels, or river networks. Fractional ADEs that can incorporate nonlocal effects in space are now used to describe anomalous transport of sediment which can arise from particle size (Foufoula-Georgiou et al., submitted manuscript, 2009a; Hill et al., submitted manuscript, 2009)

and flow field variation [*Stark et al.*, 2009; *Bradley et al.*, 2009] in streams or disturbance events on hillslopes that mobilize colluvium over a wide range of scales (Foufoula-Georgiou et al., submitted manuscript, 2009b). Fractional ADEs that incorporate nonlocal effects in time can reproduce power law residence times and loss to immobile zones that arise because tracer particles spend more time at rest than in motion at the Earth surface. These macroscopic equations arise from characteristic particle hop behaviors (Figure 11). In the Lagrangian picture, when the probability of a long hop falls off like $x^{-\alpha}$ then the α-order fractional derivative in space emerges. If the likelihood of a long residence time falls off like $t^{-\gamma}$ then a γ-fractional derivative in time appears. From an Eulerian viewpoint, fractional derivatives in space allow the possibility of high-velocity contrast, and fractional time derivatives model long power law residence times. Space or time terms in ADEs with fractional derivatives result in solutions with flexible scaling rates. In real applications, the fractional paradigm often allows the practitioner to replace scale-dependent ADE parameters by scale-independent their fADE analogues.

References

Arfken, G., and H. Weber (1995), *Mathematical Methods for Physicists*, Academic, San Diego, Calif.

Baeumer, B., and M. M. Meerschaert (2007), Fractional diffusion with two time scales, *Physica A*, *373*, 237–251.

Baeumer, B., D. Benson, and M. Meerschaert (2005), Advection and dispersion in time and space, *Physica A*, *350*, 245–262.

Benson, D. A. (1998), The fractional advection-dispersion equation: Development and application, Ph.D. dissertation, Univ. of Nev., Reno.

Benson, D. A., S. W. Wheatcraft, and M. M. Meerschaert (2000a), The fractional-order governing equation of Lévy motion, *Water Resour. Res.*, *36*(6), 1413–1423.

Benson, D. A., S. W. Wheatcraft, and M. M. Meerschaert (2000b), Application of a fractional advection-dispersion equation, *Water Resour. Res.*, *36*(6), 1403–1412.

Benson, D. A., R. Schumer, M. M. Meerschaert, and S. W. Wheatcraft (2001), Fractional dispersion, Lévy motion, and the MADE tracer tests, *Transp. Porous Media*, *42*, 211–240.

Berkowitz, B., J. Klafter, R. Metzler, and H. Scher (2002), Physical pictures of transport in heterogeneous media: Advection-dispersion, random-walk, and fractional derivative formulations, *Water Resour. Res.*, *38*(10), 1191, doi:10.1029/2001WR001030.

Berkowitz, B., A. Cortis, M. Dentz, and H. Scher (2006), Modeling non-Fickian transport in geological formations as a continuous time random walk, *Rev. Geophys.*, *44*, RG2003, doi:10.1029/2005RG000178.

Bradley, D. N., G. E. Tucker, and D. A. Benson (2009), Fractional dispersion in a sand-bed river, *J. Geophys. Res.*, doi:10.1029/2009JF001268, in press.

Clarke, D. D., M. M. Meerschaert, and S. W. Wheatcraft (2005), Fractal travel time estimates for dispersive contaminants, *Ground Water*, *43*(3), 401–407.

Coats, K. H., and B. Smith (1964), Dead-end pore volume and dispersion in porous media, *Soc. Pet. Eng. J.*, *4*, 73–84.

Culling, W. (1960), Analytical theory of erosion, *J. Geol.*, *68*, 336–344.

Cushman, J. H. (1997), *The Physics of Fluids in Hierarchical Porous Media: Angstroms to Miles*, Kluwer Acad., New York.

Cushman, J. H., and T. R. Ginn (1993), Nonlocal dispersion in media with continuously evolving scales of heterogeneity, *Transp. Porous Media*, *13*, 123–138.

Cushman, J. H., and T. R. Ginn (2000), Fractional advection-dispersion equation: A classical mass balance with convolution-Fickian flux, *Water Resour. Res.*, *36*(12), 3763–3766.

Einstein, H. (1937), Bed load transport as a probability problem (in German), Ph.D. thesis, Eidg. Tech. Hochsch., Zurich, Switzerland. (English translation by W. W. Sayre, in *Sedimentation*, edited by H. W. Shen, pp. C1–C105, Fort Collins, Colo., 1972.)

Feller, W. (1971), *An Introduction to Probability Theory and Its Applications*, Wiley Ser. Probab. Math. Stat., vol. 2, 2nd ed., John Wiley, New York.

Furbish, D. J., E. M. Childs, P. K. Haff, and M. W. Schmeeckle (2009a), Rain splash of soil grains as a stochastic advection-dispersion process, with implications for desert plant-soil interactions and land-surface evolution, *J. Geophys. Res.*, *114*, F00A03, doi:10.1029/2009JF001265.

Furbish, D. J., P. K. Haff, W. E. Dietrich, and A. M. Heimsath (2009b), Statistical description of slope-dependent soil transport and the diffusion-like coefficient, *J. Geophys. Res.*, *114*, F00A05, doi:10.1029/2009JF001267.

Ganti, V., A. Singh, P. Passalacqua, and E. Foufoula-Georgiou (2009), Subordinated Brownian motion model for sediment transport, *Phys. Rev. E*, *80*, 011111, doi:10.1103/PhysRevE.80.011111.

Gnedenko, B. V., and A. N. Kolmogorov (1968), *Limit Distributions for Sums of Independent Random Variables*, translated from Russian by K. L. Chung, Addison-Wesley, Reading, Mass.

Gooseff, M. N., S. M. Wondzell, R. Haggerty, and J. Anderson (2003), Comparing transient storage modeling and residence time distribution (RTD) analysis in geomorphically varied reaches in the Lookout Creek basin, Oregon, USA, *Adv. Water Resour.*, *26*, 925–937.

Haggerty, R., and S. M. Gorelick (1995), Multiple-rate mass transfer for modeling diffusion and surface reactions in media with pore-scale heterogeneity, *Water Resour. Res.*, *31*(10), 2383–2400.

Haggerty, R., S. A. McKenna, and L. C. Meigs (2000), On the late-time behavior of tracer test breakthrough curves, *Water Resour. Res.*, *36*(12), 3467–3479.

Haggerty, R., S. M. Wondzell, and M. A. Johnson (2002), Power-law residence time distribution in the hyporheic zone of a 2nd-order mountain stream, *Geophys. Res. Lett.*, *29*(13), 1640, doi:10.1029/2002GL014743.

Hassan, M. A., and M. Church (1992), The movement of individual grains on the streambed, in *Dynamics of Gravel-Bed Rivers*, edited by P. Billi et al., pp. 159–175, Wiley, Chichester, U. K.

Klafter, J., and R. Silbey (1980), Derivation of continuous-time random walk equation, *Phys. Rev. Lett.*, *44*(2), 55–58.

Leopold, L., M. Wolman, and J. Miller (1964), *Fluvial Processes in Geomorphology*, W. H. Freeman, San Francisco, Calif.

Mainardi, F. (1997), Fractional calculus: Some basic problems in continuum and statistical mechanics, in *Fractals and Fractional Calculus in Continuum Mechanics*, edited by A. Carpinteri and F. Mainardi, pp. 292–348, Springer, New York.

Mainardi, F., and R. Gorenflo (2000), On Mittag-Leffler-type functions in fractional evolution processes, *J. Comput. Appl. Math.*, *118*, 283–299.

Malmon, D. V., T. Dunne, and S. L. Reneau (2002), Predicting the fate of sediment and pollutants in river floodplains, *Environ. Sci. Technol.*, *36*(9), 2026–2032.

Malmon, D. V., T. Dunne, and S. L. Reneau (2003), Stochastic theory of particle trajectories through alluvial valley floors, *J. Geol.*, *111*, 525–542.

Mandelbrot, B. B. (1982), *The Fractal Geometry of Nature*, W. H. Freeman, San Francisco, Calif.

Meerschaert, M. M., and H.-P. Scheffler (2002), Semistable Lévy motion, *Fractional Calculus Appl. Anal.*, *5*, 27–54.

Meerschaert, M. M., and H.-P. Scheffler (2004), Limit theorems for continuous-time random walks with infinite mean waiting times, *J. Appl. Probab.*, *41*, 623–638.

Meerschaert, M. M., and C. Tadjeran (2004), Finite difference approximations for fractional advection-dispersion flow equations, *J. Comput. Appl. Math.*, *172*, 65–77.

Meerschaert, M. M., D. A. Benson, H.-P. Scheffler, and P. Becker-Kern (2002a), Governing equations and solutions of anomalous random walk limits, *Phys. Rev. E*, *66*, 060102, doi:10.1103/PhysRevE.66.060102.

Meerschaert, M. M., D. A. Benson, H.-P. Scheffler, and B. Baeumer (2002b), Stochastic solution of space-time fractional diffusion equations, *Phys. Rev. E*, *65*, 041103, doi:10.1103/PhysRevE.65.041103.

Meerschaert, M. M., J. Mortensen, and S. W. Wheatcraft (2006), Fractional vector calculus for fractional advection-dispersion, *Physica A*, *367*, 181–190.

Montroll, E. W., and G. H. Weiss (1965), Random walks on lattices. II, *J. Math. Phys.*, *6*(2), 167–181.

Neuman, S. P. (1990), Universal scaling of hydraulic conductivities and dispersivities in geologic media, *Water Resour. Res.*, 26(8), 1749–1758.

Neuman, S. P., and D. M. Tartakovsky (2009), Perspective on theories of non-Fickian transport in heterogeneous media, *Adv. Water Resour.*, 32, 670–680.

Nikora, V., H. Habersack, T. Huber, and I. McEwan (2002), On bed particle diffusion in gravel bed flows under weak bed load transport, *Water Resour. Res.*, 38(6), 1081, doi:10.1029/2001WR000513.

Nolan, J. P. (1998), Multivariate stable distributions: Approximation, estimation, simulation and identification, in *A Practical Guide to Heavy Tails: Statistical Techniques and Applications*, edited by R. Adler, R. Feldman, and M. Taqqu, pp. 509–526, Birkhäuser, Boston, Mass.

Parker, G., C. Paola, and S. Leclair (2000), Probabilistic Exner sediment continuity equation for mixtures with no active layer, *J. Hydraul. Eng.*, 126(11), 818–826.

Pryce, R. S., and P. E. Ashmore (2003), The relation between particle path length distributions and channel morphology in gravel-bed streams: A synthesis, *Geomorphology*, 56, 167–187.

Sadler, P. M. (1981), Sediment accumulation rates and the completeness of stratigraphic sections, *J. Geol.*, 89, 569–584.

Samko, S. G., A. A. Kilbas, and O. I. Marichev (1993), *Fractional Integrals and Derivatives: Theory and Applications*, Gordon and Breach, London.

Samorodnitsky, G., and M. S. Taqqu (1994), *Stochastic Modeling, Stable Non-Gaussian Random Processes: Stochastic Models With Infinite Variance*, Chapman and Hall, London.

Sayre, W., and D. Hubbell (1965), Transport and dispersion of labeled bed material: North Loup River, Nebraska, *U.S. Geol. Surv. Prof. Pap., 433-C*.

Scher, H., and M. Lax (1973), Stochastic transport in a disordered solid. I. Theory, *Phys. Rev. B*, 7(10), 4491–4502.

Schumer, R., and D. J. Jerolmack (2009), Real and apparent changes in sediment deposition rates through time, *J. Geophys. Res.*, 114, F00A06, doi:10.1029/2009JF001266.

Schumer, R., D. A. Benson, M. M. Meerschaert, and S. W. Wheatcraft (2001), Eulerian derivation for the fractional advection-dispersion equation, *J. Contam. Hydrol.*, 48, 69–88.

Schumer, R., D. A. Benson, M. M. Meerschaert, and B. Baeumer (2003), Fractal mobile/immobile solute transport, *Water Resour. Res.*, 39(10), 1296, doi:10.1029/2003WR002141.

Singh, A., K. Fienberg, D. J. Jerolmack, J. Marr, and E. Foufoula-Georgiou (2009), Experimental evidence for statistical scaling and intermittency in sediment transport rates, *J. Geophys. Res.*, 114, F01025, doi:10.1029/2007JF000963.

Stark, C. P., E. Foufoula-Georgiou, and V. Ganti (2009), A nonlocal theory of sediment buffering and bedrock channel evolution, *J. Geophys. Res.*, 114, F01029, doi:10.1029/2008JF000981.

Tadjeran, C., M. M. Meerschaert, and H.-P. Scheffler (2006), A second order accurate numerical approximation for the fractional diffusion equation, *J. Comput. Phys.*, 213, 205–213.

Tipper, J. C. (1983), Rates of sedimentation and stratigraphical completeness, *Nature*, 302(5910), 696–698.

Wörman, A., A. I. Packman, L. Marklund, J. W. Harvey, and S. H. Stone (2007), Fractal topography and subsurface water flows from fluvial bedforms to the continental shield, *Geophys. Res. Lett.*, 34, L07402, doi:10.1029/2007GL029426.

Zhang, Y., D. A. Benson, and B. Baeumer (2008), Moment analysis for spatiotemporal fractional dispersion, *Water Resour. Res.*, 44, W04424, doi:10.1029/2007WR006291.

————————————

B. Baeumer, Department of Mathematics and Statistics, University of Otago, PO Box 56, Dunedin 9054, New Zealand. (bbaeumer@maths.otago.ac.nz)

M. M. Meerschaert, Department of Statistics and Probability, Michigan State University, East Lansing, MI 48824, USA. (mcubed@stt.msu.edu)

R. Schumer, Division of Hydrologic Sciences, Desert Research Institute, Reno, NV 89512, USA. (rina@dri.edu)